Hydrodynamic stability of viscous flow between rotating porous cylinders with radial flow

Kyungyoon Min and Richard M. Lueptow
Department of Mechanical Engineering, Northwestern University, Evanston, Illinois 60208

(Received 28 January 1993; accepted 1 September 1993)

A linear stability analysis has been carried out for flow between porous concentric cylinders when radial flow is present. Several radius ratios with corotating and counter-rotating cylinders were considered. The radial Reynolds number, based on the radial velocity at the inner cylinder and the inner radius, was varied from -30 to 30. The stability equations form an eigenvalue problem that was solved using a numerical technique based on the Runge–Kutta method combined with a shooting procedure. The results reveal that the critical Taylor number at which Taylor vortices first appear decreases and then increases as the radial Reynolds number becomes more positive. The critical Taylor number increases as the radial Reynolds number becomes more negative. Thus, radially inward flow and strong outward flow have a stabilizing effect, while weak outward flow has a destabilizing effect on the Taylor vortex instability. Profiles of the relative amplitude of the perturbed velocities show that radially inward flow shifts the Taylor vortices toward the inner cylinder, while radially outward flow shifts the Taylor vortices toward the outer cylinder. The shift increases with the magnitude of the radial Reynolds number and as the annular gap widens.

I. INTRODUCTION

The stability of flow in the annulus between concentric, differentially rotating cylinders has been studied for many years from both theoretical and experimental points of view. Taylor[1] analytically predicted the onset of the instability of circular Couette flow and conducted a simple flow visualization experiment to confirm his prediction. The instability appears as counter-rotating, toroidal vortices stacked in the annulus. Chandrasekhar[2] and DiPrima and Swinney[3] provide extensive summaries of the abundant research on this subject since Taylor's pioneering work.

The stability of Taylor vortex flow is altered when an additional flow is superimposed on the circular Couette flow. For instance, an axial flow in the annulus stabilizes the circular Couette flow, so that the transition to Taylor vortex flow occurs at a higher Taylor number.[4–7] The axial flow can also alter the character of the flow instability.[8] However, little information is available about how radial flow in the annulus affects the stability of the Taylor vortex flow. This type of flow occurs during dynamic filtration using a rotating filter.[9,10] In these filtration devices a suspension is contained between a rotating porous inner cylinder and a stationary nonporous outer cylinder. Filtrate passes radially through the porous wall of the rotating inner cylinder, while the concentrate is retained in the annulus. The Taylor vortices appearing in the device are believed to wash the filter surface of the inner cylinder clean of particles, preventing the plugging of pores of the filter medium with particles.[11]

The purpose of this study is to determine the effect of a radial flow on the stability of the flow and relative amplitude of the perturbed velocities. In particular, we use linear stability analysis to determine the critical Taylor number and associated wave number for the transition from stable circular Couette flow to Taylor vortex flow when there is a radial flow between two concentric, porous, differentially rotating cylinders. The results of the stability analysis are used to determine the relative amplitude of the perturbed velocities.

The velocity field for stable radial flow between differentially rotating porous cylinders has been investigated.[12–14] Chang and Sartory[15] considered the hydromagnetic stability of an electrically conducting fluid between porous concentric cylinders with a wide gap between the cylinders. Although they were primarily concerned with the asymptotic behavior of the flow at large radial Reynolds numbers, they predicted that radially inward flow through the porous cylinders stabilizes the flow. Radially outward flow destabilizes the flow for weak radial flow, but stabilizes the flow for strong radial flows. Bahl[16] considered the linear hydrodynamic stability for the case where the gap between the cylinders is small compared to the radius of the cylinders, the axial wave number is fixed, and the cylinders co- or counter-rotate. His stability analysis indicated that an inward radial velocity stabilizes the flow, while an outward radial velocity destabilizes the flow. Reddy and Reddy[17] and Reddy *et al.*[18] extended Bahl's linear stability analysis to non-Newtonian fluids.[19] In contrast to Bahl, as well as Chang and Sartory, they concluded that for Newtonian fluids radial inflow destabilizes the flow, and radial outflow stabilizes the flow. But several ambiguities in their analysis hint that their results may be unreliable.

In this paper we present a linear hydrodynamic stability analysis of circular Couette flow with an imposed radial flow, as shown in Fig. 1. We consider the case of infinitely long concentric cylinders with both radial inflow and radial outflow. Unlike Bahl, we use the full linear disturbance equations and do not make the simplifying assumption of flow in a narrow gap or a specified axial wave number. While Chang and Sartory were interested in the asymptotic

 1070-6631/94/6(1)/144/8/$6.00

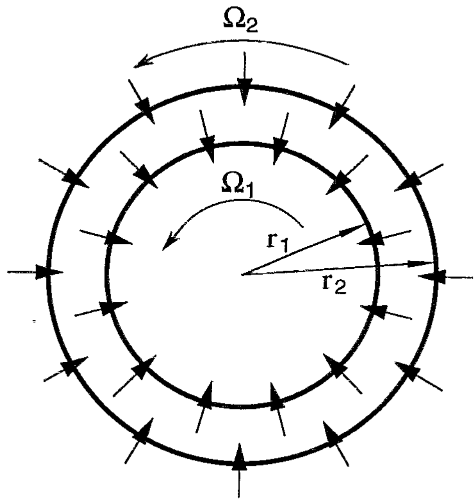

FIG. 1. Sketch of the flow configuration. The radial flow can be inward ($\alpha<0$), as shown, or outward ($\alpha>0$).

behavior of the critical Taylor number with radial Reynolds number, we consider the behavior for small radial Reynolds numbers. We also analyze corotating and counter-rotating cylinders in addition to the case of a stationary outer cylinder. Finally, in addition to the stability analysis itself, we present profiles of the relative amplitudes of the perturbed velocity for different radial flow Reynolds numbers to determine the effect of the radial flow on the position of the Taylor vortices.

II. ANALYTICAL FORMULATION

The analytical formulation of the problem was given in detail by Bahl,[16] and only the highlights are repeated here. The Navier–Stokes equation and continuity equation in cylindrical coordinates (r,θ,z) for steady, incompressible flow in the absence of a body force are used to find the stable solution for radial flow between concentric cylinders. The velocity field (U,V,W) is

$$U(r)=\frac{\alpha\nu}{r},\quad V(r)=Ar^{\alpha+1}+\frac{B}{r},\quad W=0. \tag{1}$$

Here $\alpha=u_1r_1/\nu$ is the radial Reynolds number, where u_1 is the radial velocity through the wall of the inner porous cylinder with a positive value when outward from the axis of rotation, and ν is the kinematic viscosity. The constants A and B are

$$A=\frac{-\Omega_1\eta^2(1-\mu/\eta^2)}{r_2^\alpha(1-\eta^{\alpha+2})},\quad B=r_1^2\Omega_1\frac{1-\mu\eta^\alpha}{1-\eta^{\alpha+2}}, \tag{2}$$

where $\eta=r_1/r_2$ is the radius ratio, and $\mu=\Omega_2/\Omega_1$ is the angular velocity ratio. For $\alpha=0$, the equations revert to the solution for circular Couette flow between impermeable cylinders.[2]

The stability problem is based on small perturbations of the velocity field u_r, u_θ, and u_z and the pressure field ω. The perturbations are expressed as normal modes of the form

$$u_r=e^{qt}u(r)\cos kz,\quad u_\theta=e^{qt}v(r)\cos kz,$$
$$u_z=e^{qt}w(r)\sin kz,\quad \omega=e^{qt}\omega(r)\cos kz, \tag{3}$$

where k is the axial wave number of the disturbance, q is an amplification factor, and $u(r)$, $v(r)$, $w(r)$, and $\omega(r)$ are amplitudes of the perturbation. Substitution of these quantities into the cylindrical Navier–Stokes and continuity equations followed by discarding higher-order terms, results in the following equations for the amplitudes of the perturbed quantities:

$$\nu\left(\frac{d^2u}{dr^2}+\frac{1}{r}\frac{du}{dr}-\frac{u}{r^2}-k^2u-\frac{q}{\nu}u\right)+\frac{2V}{r}v-u\frac{dU}{dr}-U\frac{du}{dr}=\frac{d\omega}{dr}, \tag{4}$$

$$\nu\left(\frac{d^2v}{dr^2}+\frac{1}{r}\frac{dv}{dr}-\frac{v}{r^2}-k^2v-\frac{q}{\nu}v\right)-\left(\frac{dV}{dr}+\frac{V}{r}\right)u$$
$$-\left(\frac{dv}{dr}+\frac{v}{r}\right)U=0, \tag{5}$$

$$\nu\left(\frac{d^2w}{dr^2}+\frac{1}{r}\frac{dw}{dr}-k^2w-\frac{q}{\nu}w\right)-U\frac{dw}{dr}=ik\omega, \tag{6}$$

$$\frac{du}{dr}+\frac{u}{r}=-ikw, \tag{7}$$

where i is the square root of -1.

Equations (6) and (7) are combined to express ω in terms of u. The resulting expression for ω is used in Eq. (4) to obtain

$$\frac{\nu}{k^2}\left(DD_*-k^2-\frac{q}{\nu}\right)(DD_*-k^2)u-\frac{1}{k^2}(DU)D(D_*u)$$
$$-\frac{1}{k^2}UD^2(D_*u)+D(uU)=\frac{2V}{r}v, \tag{8}$$

where

$$D_*=\frac{d}{dr}+\frac{1}{r},\qquad D=\frac{d}{dr}. \tag{9}$$

Equation (5) can be rewritten as

$$\nu\left(DD_*-k^2-\frac{q}{\nu}\right)v=(D_*V)u+(D_*v)U. \tag{10}$$

Here Bahl[16] used the narrow gap assumption and a fixed wave number to simplify the equations, whereas we retain all terms and do not fix the wave number. The following dimensionless length scale, wave number, amplification factor, and velocity are introduced,

$$r'=\frac{r}{r_2},\quad a=r_2k,\quad \sigma=\frac{q}{\nu}r_2^2,\quad v'=\frac{v}{r_1\Omega_1}. \tag{11}$$

Using these values along with Eq. (1) in Eq. (10) results in an expression for the amplitude of the perturbed radial velocity,

$$u=u'r_1\Omega_1 = \frac{\nu r_1\Omega_1}{(\alpha+2)Ar_2^{\alpha+2}r'^{\alpha}}\left(D'D'_*-a^2-\sigma-\frac{\alpha}{r'}D'_*\right)v'. \quad (12)$$

The amplitude of the axial perturbation velocity w can be found in terms of v' from Eqs. (7) and (12),

$$w=w'r_1\Omega_1 = \frac{\nu r_1\Omega_1}{-ia(\alpha+2)Ar_2^{\alpha+2}} \times D'_*\left[\frac{1}{r'^{\alpha}}\left(D'D'_*-a^2-\sigma-\frac{\alpha}{r'}D'_*\right)v'\right]. \quad (13)$$

Using Eqs. (1), (11), and (12) in Eq. (8) results in an expression with v' as the only dependent variable,

$$(D'D'_*-a^2-\sigma)(D'D'_*-a^2)\frac{[D'D'_*-a^2-\sigma-(\alpha/r')D'_*]v'}{r'^{\alpha}}-\frac{\alpha}{r'}D'^2\left(D'_*\frac{[D'D'_*-a^2-\sigma-(\alpha/r')D'_*]v'}{r'^{\alpha}}\right)$$
$$-\alpha D'\left(\frac{1}{r'}\right)D'\left(D'_*\frac{[D'D'_*-a^2-\sigma-(\alpha/r')D'_*]v'}{r'^{\alpha}}\right)+a^2\alpha\frac{[D'D'_*-a^2-\sigma-(\alpha/r')D'_*]v'}{r'^{\alpha}}D'\left(\frac{1}{r'}\right)$$
$$+\frac{a^2\alpha}{r'}D'\left(\frac{[D'D'_*-a^2-\sigma-(\alpha/r')D'_*]v'}{r'^{\alpha}}\right)=-Tr'^{\alpha}\left(\frac{1}{r'^{\alpha+2}}-\kappa\right)a^2v', \quad (14)$$

where κ is a parameter related to the radius ratio and angular velocity ratio, such that

$$\kappa=\frac{(1-\mu/\eta^2)}{(1-\mu\eta^{\alpha})}, \quad (15)$$

and T is a special form of the Taylor number specific to this problem,

$$T=\mathrm{Ta}^2\frac{2(\alpha+2)\eta^2(1-\mu/\eta^2)(1-\mu\eta^{\alpha})}{(1-\eta^{\alpha+2})^2(1-\eta)^2}. \quad (16)$$

The dimensionless parameter T is expressed in terms of a simple form of the Taylor number, sometimes referred to as the rotating Reynolds number, $\mathrm{Ta}=\Omega_1 r_1(r_2-r_1)/\nu$.

The perturbation velocity amplitudes u', v', and w' must vanish on the boundaries at $r'=\eta$ and $r'=1$. Using Eqs. (12) and (13) the boundary conditions on the three perturbation velocity amplitudes can be written in terms of v' as

$$\left(D'D'_*-a^2-\sigma-\frac{\alpha}{r'}D'_*\right)v'=0, \quad (17a)$$

$$v'=0, \quad (17b)$$

$$D'_*\left[\frac{1}{r'^{\alpha}}\left(D'D'_*-a^2-\sigma-\frac{\alpha}{r'}D'_*\right)v'\right]=0. \quad (17c)$$

Equation (14) is a sixth-order ordinary differential equation for which the amplification factor σ is set to zero at the onset of the instability. Equation (14) subject to boundary conditions (17) leads to an eigenvalue problem. To solve the problem we used a shooting method similar to the one used by Sparrow *et al.*[20] First, a trial value of Ta was selected. Then three trial solutions, v_{I}, v_{II}, and v_{III}, were constructed that satisfy Eq. (14) for prescribed values of α, a, η, and μ. All three trial solutions satisfied the boundary condition at the inner wall (17) for v', d^2v'/dr'^2, and d^3v'/dr'^3. But each trial solution satisfied a different set of boundary conditions for dv'/dr', d^4v'/dr'^4, and d^5v'/dr'^5 at the inner wall, accomplished by setting one of these three boundary conditions to unity and the remaining two to zero. A forward integration scheme was used to compute each trial solution using the six initial conditions at $r'=\eta$ for each of the trial solutions. In general, none of the trial solutions satisfied the boundary conditions at $r'=1$, so a linear combination of the trial solutions provided the final solution,

$$v'=c_1v_{\mathrm{I}}+c_2v_{\mathrm{II}}+c_3v_{\mathrm{III}}. \quad (18)$$

The three coefficients, c_1, c_2, and c_3, were found from the linear combination of the three boundary conditions (17) at the outer wall. This linear combination of boundary conditions resulted in a three by three matrix of values, one for each combination of boundary condition and trial solution, which must have a zero determinant to obtain a nontrivial solution. For any trial value of Ta along with prescribed values of α, a, η, and μ, this determinant was not necessarily zero, so the operations described above were repeated for a series of trial values of Ta until one was found for which the determinant of the coefficients was zero. Then, the wave number a was varied and the process described above was repeated until the critical wave number for which Ta is a minimum was found. This minimum Taylor number is the critical Taylor number, Ta_c.

Once the values of c_1, c_2, and c_3 were determined, u', v', and w' were found from (12), (18), and (13), respectively. Since the three boundary conditions at the outer wall are all zero, only the ratio between c_1, c_2, and c_3 could be calculated. Thus, only the relative values of u, v, and w, not their absolute magnitudes, could be determined.

TABLE I. Comparison of the critical Taylor number and wave number with previous results.

Radius ratio η	Ref. 21 Ta_c	Ref. 21 a	Ref. 6 Ta_c	Ref. 6 a	Present results Ta_c	Present results a
0.95	184.98	3.128	184.99	3.128	184.99	3.128
0.90	131.61	3.129	···	···	131.62	3.129
0.85	108.31	3.130	···	···	108.32	3.131
0.75	85.78	3.136	85.78	3.135	85.78	3.135
0.50	68.186	3.163	68.189	3.151	68.188	3.162

For the results described here, Eq. (14) was solved numerically using a fourth-order Runge–Kutta method with 21 points to span the gap between the inner and outer cylinders. The radial Reynolds number α was varied from -30 to 30 in increments of 0.5 near $\alpha=0$ and increments of 5 for $|\alpha|>5$, avoiding a singularity at $\alpha=-2$. The angular velocity ratio μ was varied from -0.2 to 0.3 in increments of 0.1. The problem was solved for five radius ratios η of 0.50, 0.75, 0.85, 0.90, and 0.95.

To assure the validity of our procedure we compared our results to previously published results[6,21] for the case of no radial flow ($\alpha=0$). The similarity of the values for the critical Taylor number Ta_c and the critical wave number a, shown in Table I, confirm that our procedure is correct.

III. RESULTS AND DISCUSSION

The effect of radial flow on the stability of Taylor–Couette flow is shown in Fig. 2(a) for the case of the outer cylinder fixed and the inner cylinder rotating. Radial inflow, corresponding to negative Reynolds numbers, increases the critical Taylor number for all radius ratios shown, indicating a stabilizing effect. Radial outflow also stabilizes the flow by increasing the critical Taylor number for large positive Reynolds numbers. However, for small positive Reynolds numbers the critical Taylor number decreases indicating less stable flow, as shown in Fig. 2(b). The upturn in the curve related to the stabilizing effect of strong radially outward flows is already evident for $\eta=0.50$ and $\eta=0.75$. For narrower gaps the increased stability due to strong radial outflow is delayed to higher α. Bahl[16] found a similar result over the narrow range of radial Reynolds numbers that he considered for the limiting case of η approaching unity. For narrow gaps, indicated by radius ratios near unity, varying the radial Reynolds number has a relatively small effect on the critical Taylor number. As the annular gap widens, indicated by decreasing radius ratios, the effect of the radial flow has a more dramatic effect on the critical Taylor number. Similar results were obtained by Chang and Sartory,[15] although direct comparison is difficult.

When the outer cylinder is co- or counter-rotating with respect to the inner cylinder, the effect of radial flow on the stability of the flow is similar to the case of a stationary outer cylinder. The effect of varying $\mu=\Omega_2/\Omega_1$ on the stability of the flow for a radius ratio $\eta=0.85$ over a range of Reynolds numbers near zero is shown in Fig. 3(a). In all cases, the flow in the annulus is more stable for radially

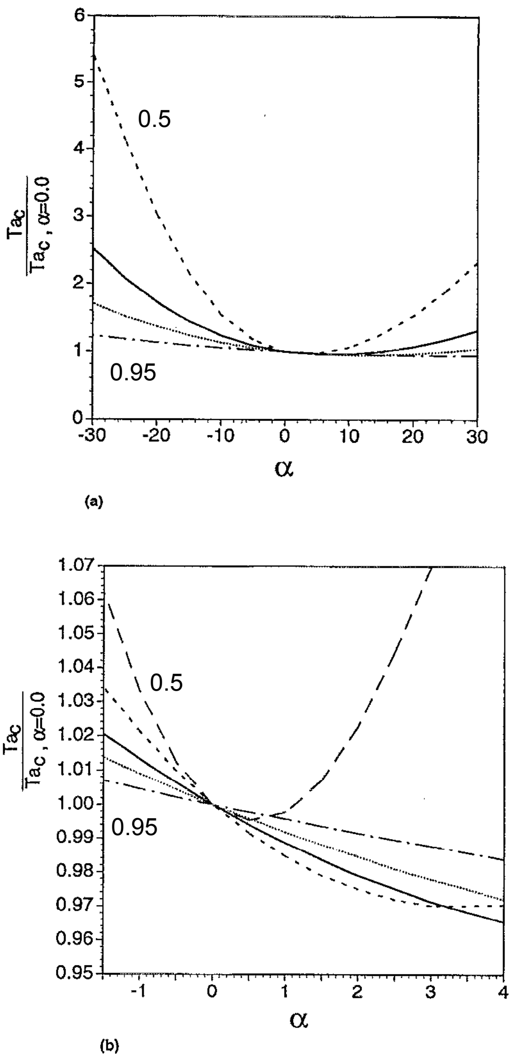

FIG. 2. The effect of the radial Reynolds number α on the critical Taylor number, Ta_c, for transition to vortex flow normalized by the critical Taylor number for no radial flow, $\mathrm{Ta}_{c,\alpha=0}$ - - -, $\eta=0.95$; ···, $\eta=0.9$; ——, $\eta=0.85$; ---, $\eta=0.75$; and – – –, $\eta=0.5$. The outer cylinder is stationary ($\mu=0$). (a) Over the entire range of study, $-30<\alpha<30$. (b) Detail for $-1.5\leq\alpha\leq4$.

inward flow through the porous walls than radially outward flow. For identical absolute values of μ, the transition to Taylor vortex flow occurs at higher Taylor number for flow between corotating cylinders than for flow between counter-rotating cylinders. Varying the radial Reynolds number only changes the critical Taylor number slightly for corotating cylinders. The effect of changing the radial Reynolds number is greater for counter-rotating cylinders.

As is the case with no radial flow, the axial wave number of the vortices a is always larger for counter-rotating cylinders than for corotating cylinders, independent of radial Reynolds number, as shown in Fig. 3(b). The appearance of the curves suggests that as the radial Reynolds number increases, the wave number may asymptote to a particular value, independent of μ.

The effect of the radial flow on the relative amplitude of the perturbed velocities is shown in Fig. 4 for $\eta=0.85$ with a stationary outer cylinder ($\mu=0$). The relative am-

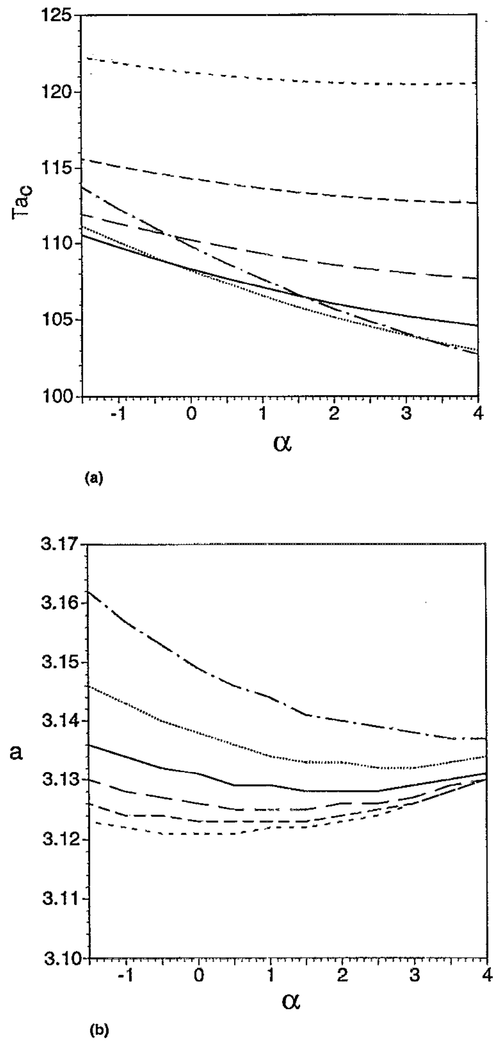

FIG. 3. (a) The effect of radial Reynolds number α and angular velocity ratio μ on the critical Taylor number Ta_c for $\eta=0.85$. (b) The effect of radial Reynolds number α and angular velocity ratio μ on the critical wave number a for $\eta=0.85$. - - -, $\mu=0.3$; — — —, $\mu=0.2$; — — —, $\mu=0.1$; ——, $\mu=0$; $\cdots$, $\mu=-0.1$; and — - —, $\mu=-0.2$.

plitudes shown in the figure can be related to the perturbed velocities through Eq. (3). Since the scaling of the amplitudes of the perturbed velocity components cannot be determined with respect to the velocity scale of the problem, the amplitudes are normalized by the maximum amplitude of the perturbed azimuthal velocity component, $v_{\max}$, for that particular radial Reynolds number. The amplitudes of the perturbed velocities are zero at the inner wall, $r'=\eta$, and at the outer wall, $r'=1$, in keeping with the proper boundary conditions at the wall.

The radial position of the maximum value of the relative amplitude of the perturbed azimuthal velocity v is shifted depending upon the radial Reynolds numbers, as shown in Fig. 4(a). For radially inward flow the maximum is shifted toward the inner cylinder, and for radially outward flow the maximum is shifted toward the outer cylinder. The shifting of the maximum is also evident for the relative amplitude of the perturbed radial velocity u, as shown in Fig. 4(b). The relative amplitude of the per-

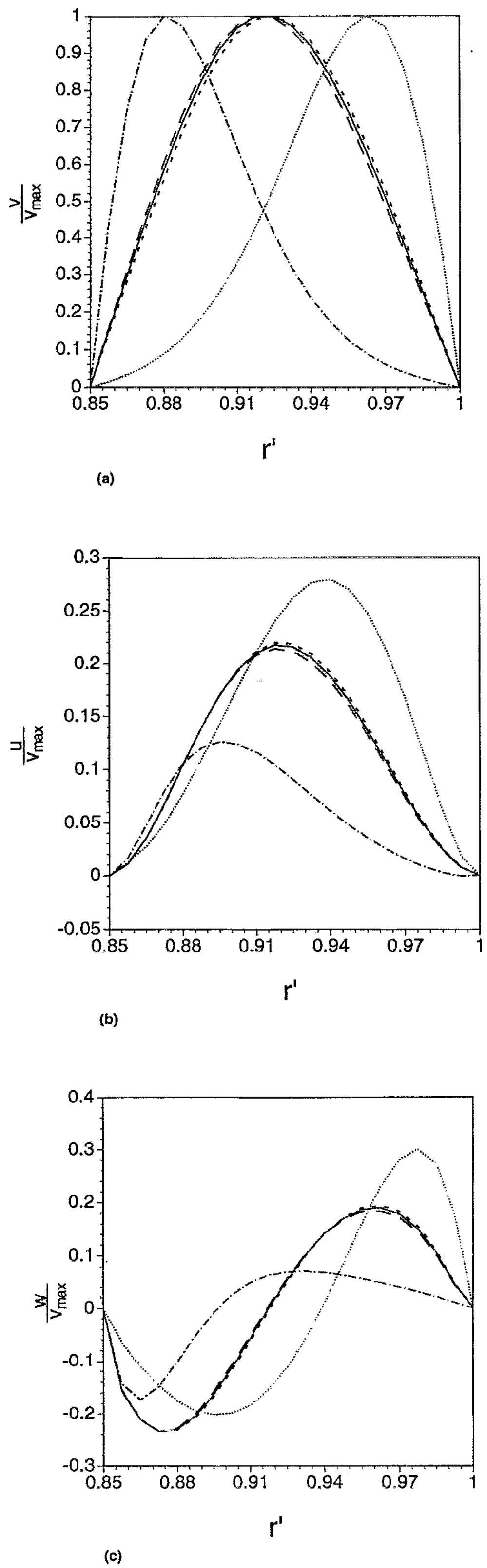

FIG. 4. The relative amplitude of the perturbation velocity from the inner cylinder at $r'=0.85$ to the outer cylinder at $r'=1$ for $\eta=0.85$ and $\mu=0$. - - -, $\alpha=-30$ (radially inward flow); — — —, $\alpha=-1$; ——, $\alpha=0$ (no radial flow); ---, $\alpha=1$ (radially outward flow); $\cdots$, $\alpha=30$. (a) Relative amplitude of azimuthal perturbation velocity $v/v_{\max}$. (b) Relative amplitude of radial perturbation velocity $u/v_{\max}$. (c) Relative amplitude of axial perturbation velocity $w/v_{\max}$.

turbed radial velocity is less than one-third that of the azimuthal velocity. Radially inward flow results in a greater suppression of the relative amplitude of the radial velocity than radially outward flow. The relative amplitude of the perturbed axial velocity w is shown in Fig. 4(c). The sinusoidal shape of the curves is consistent with axial flow in opposite directions at the inner and outer portions of the Taylor vortex. Again the relative amplitude of the axial velocity component is less than one-third that of the azimuthal velocity, and radially inward flow suppresses the amplitude more than radially outward flow. The zero crossing, maxima, and minima are shifted inward for radially inward flow and outward for radially outward flow.

Clearly, the radial flow shifts the position of the vortex within the annular gap between the cylinders. The shift in the radial position of the vortex is quite evident in the perturbed u-w velocity vector plots shown in Fig. 5. In the case of no radial flow, Fig. 5(b), the vortex is almost centered in the annular gap. The radial flow shifts the vortex in the direction of the flow, as shown in Figs. 5(a) and 5(c). The radial flow also acts to increase the wavelength of the vortices, evident as elongated vortices in Figs. 5(a) and 5(c). The axial wavelength of the vortices is a minimum near values of α slightly greater than zero for all cases considered.

The effect of the radius ratio on the shifting of the vortex is shown in Fig. 6 for the relative amplitude of the perturbed azimuthal velocity. For a wide annular gap between the two cylinders corresponding to $\eta=0.75$, the radial shift of the maximum of the relative amplitude of the perturbed velocity is much greater than for a narrower gap corresponding to $\eta=0.95$. The case of $\eta=0.85$, shown in Fig. 4(a), falls in between. The profiles of the relative amplitudes u and w show similar trends. The greater radial shift of the Taylor vortex in a wide annular gap than in a narrow annular gap may be a simple result of there being little room in a narrow gap annulus for the vortex to shift radially compared to a wide gap.

The angular velocity ratio μ has only a small effect on the radial shift of the vortex. In Fig. 7 the relative amplitude of the perturbed azimuthal velocity is plotted for $\mu=-0.2$ and $\mu=0.2$ in the case of $\eta=0.85$. For both radially inward flow ($\alpha=-1$) and radially outward flow ($\alpha=4$), counter-rotating cylinders results in the curves shifting slightly inward, and corotating cylinders results in the curves shifting slightly outward. The same result occurs for no radial flow.

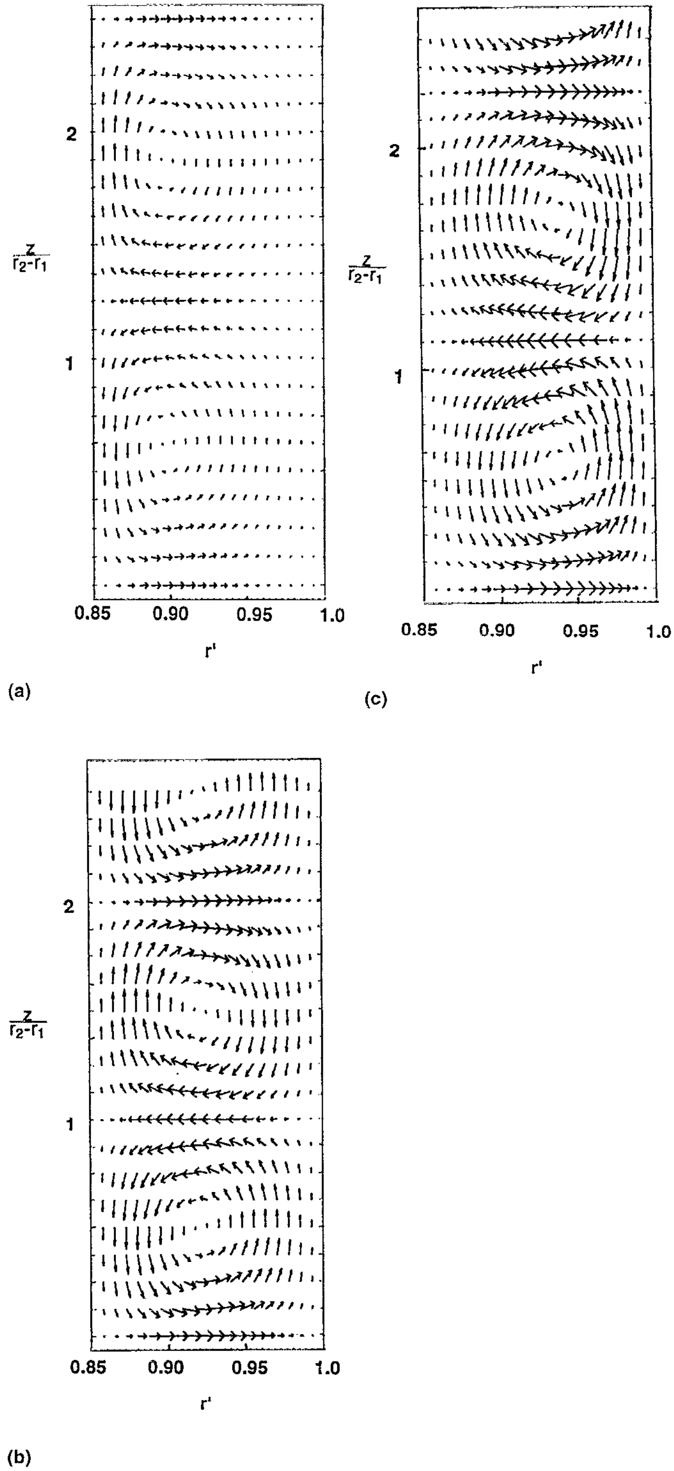

FIG. 5. Velocity vector plots in a radial plane for $\eta=0.85$. The inner cylinder is at $r'=0.85$ and the outer cylinder is at $r'=1$. The vertical dimension z is normalized by the gap width r_2-r_1. (a) $\alpha=-30$. (b) $\alpha=0$. (c) $\alpha=30$.

IV. SUMMARY

The results of this analysis of flow between differentially rotating porous cylinders indicate that radially inward flow stabilizes the flow, whereas weak radially outward flow destabilizes the flow. This result is true regardless of radius ratio, although the effect is greater than the radius ratio is decreased. The stability result is also independent of whether the cylinders are co- or counter-rotating. Although a weak radial outflow destabilizes the flow, a strong outflow stabilizes the flow.

The physical effect of radial flow on the transition from stable flow to supercritical vortex flow may be related to where the incipient instability appears in the annulus. When there is no radial flow and the outer cylinder is fixed, the instability first appears near the inner rotating cylinder and propagates radially outward as the Taylor number

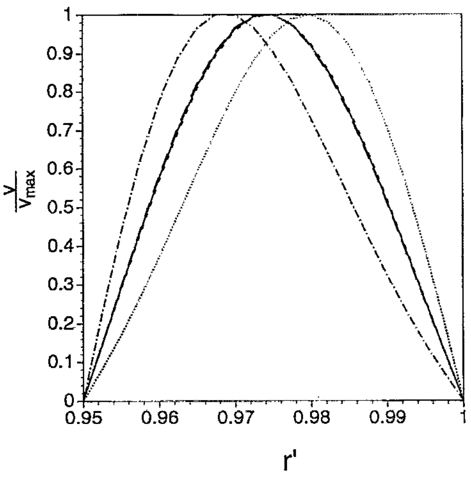

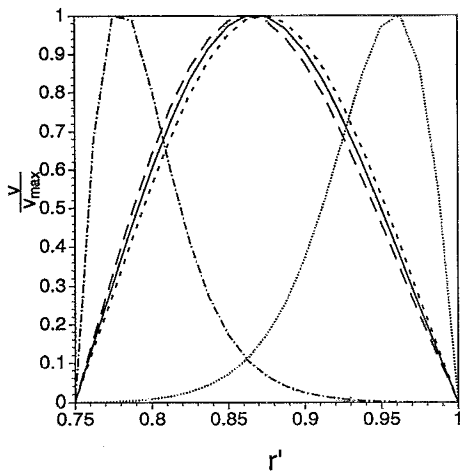

FIG. 6. The relative amplitude of the azimuthal perturbation velocity from the inner cylinder to the outer cylinder for $\mu=0$. (a) $\eta=0.75$. (b) $\eta=0.95$. The curves are identified in Fig. 4.

increases.[22,23] When a radial inflow is imposed, it may wash the fluid where the incipient instability first appears out of the annulus through the porous inner cylinder increasing the Taylor number at which the instability will occur throughout the entire annulus. On the other hand, a weak radial outflow washes the instability from near the inner cylinder outward across the annulus, resulting in the supercritical transition at a lower Taylor number. But if the outflow is strong enough, it overwhelms the centrifugal instability, delaying the onset of supercritical vortices.

The vortices in the annulus are shifted as a result of the radial flow, with the largest shifts occurring for the largest magnitudes of the radial Reynolds numbers. Radially inward flow shifts the vortices inward, while radially outward flow shifts the vortices outward. The shift is greater for a wide gap between the cylinders than for a narrow gap.

The original motivation for this work was the flow in a rotating filter device. In such a device, only the inner cylinder is porous, while the outer cylinder is nonporous. An

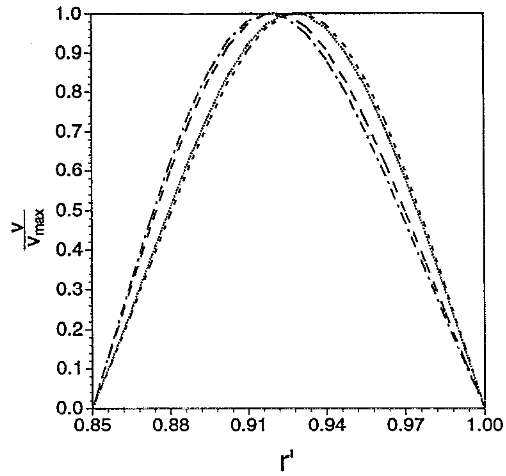

FIG. 7. The relative amplitude of the azimuthal perturbation velocity from the inner cylinder to the outer cylinder for $\eta=0.85$. – – –, $\mu=0.2$, $\alpha=-1$; - - -, $\mu=-0.2$, $\alpha=-1$; ---, $\mu=0.2$, $\alpha=4$; and $\cdots$, $\mu=-0.2$, $\alpha=4$.

axial flow in the annulus is the source of the fluid that flows radially inward through the inner porous cylinder. The case of a single porous rotating cylinder, such as that in a rotating filter, is not as easily amenable to analysis as the flow discussed in this paper because no analytic stable solution exists for the flow and because the flow through the porous inner cylinder varies with axial position. However, the results presented here suggest several comments that can be made with respect to the rotating filter application. Since the bulk radial flow in a rotating filter is radially inward, results here suggest that a slightly higher rotational speed is needed to assure the appearance of Taylor vortices in the annulus than if there were no radial flow. The inward radial flow also shifts the vortices inward toward the porous inner cylinder. Most likely, this will have an advantageous effect on the role of Taylor vortices in washing the surface of the inner cylinder clean of particles preventing the pores of the rotating filter from plugging.

ACKNOWLEDGMENT

The support of The Whitaker Foundation is gratefully acknowledged.

[1] G. I. Taylor, "Stability of a viscous liquid contained between two rotating cylinders," Philos. Trans. R. Soc. London Ser. A **223**, 289 (1923).

[2] S. Chandrasekhar, *Hydrodynamic and Hydromagnetic Stability* (Oxford U. P., Oxford, 1961), pp. 272–342.

[3] R. C. DiPrima and H. L. Swinney, "Instabilities and transition in flow between concentric rotating cylinders," in *Topics in Applied Physics, Hydrodynamic Instabilities and the Transition to Turbulence*, edited by H. L. Swinney and J. P. Gollub (Springer-Verlag, Berlin, 1985), pp. 139–180.

[4] S. Chandrasekhar, "The hydrodynamic stability of viscid flow between coaxial cylinders," Proc. Natl. Acad. Sci. **46**, 141 (1960).

[5] R. C. DiPrima, "The stability of a viscous fluid between rotating cylinders with an axial flow," J. Fluid Mech. **9**, 621 (1960).

[6] K. C. Chung and K. N. Astill, "Hydrodynamic instability of viscous flow between rotating coaxial cylinders with fully developed axial flow," J. Fluid Mech. **81**, 641 (1977).

[7]K. L. Babcock, G. Ahlers, and D. S. Cannell, "Noise-sustained structure in Taylor–Couette flow with through flow," Phys. Rev. Lett. **67**, 3392 (1991).

[8]R. M. Lueptow, A. Docter, and K. Min, "Stability of axial flow in an annulus with a rotating inner cylinder," Phys. Fluids A **4**, 2446 (1992).

[9]K. H. Kroner, V. Nissinen, and H. Ziegler, "Improving dynamic filtration of microbial suspensions," Biotechnology **5**, 921 (1987).

[10]S. Wronski, E. Molga, and L. Rudniak, "Dynamic filtration in biotechnology," Bioprocess Eng. **4**, 99 (1989).

[11]J. R. Hildebrandt and J. B. Saxton, "The use of Taylor vortices in protein processing to enhance membrane filtration performance," *Bioprocess Engineering Colloquium*, edited by R. C. Dean and R. M. Nerem (ASME, New York, 1987), ASME Book No. G00422, pp. 93–96.

[12]S. P. Mishra and J. S. Roy, "Flow of elasticoviscous liquid between rotating cylinders with suction and injection," Phys. Fluids **11**, 2074 (1968).

[13]J. R. Mahapatra, "A note on the unsteady motion of a viscous conducting liquid between two porous concentric circular cylinders acted on by a radial magnetic field," Appl. Sci. Res. **27**, 274 (1973).

[14]P. G. Bellamy-Knights and R. Saci, "Viscous vortex core generation," Acta Mech. **67**, 121 (1987).

[15]T. S. Chang and W. K. Sartory, "Hydromagnetic stability of dissipative flow between rotating permeable cylinders: Part 1. Stationary critical modes," J. Fluid Mech. **27**, 65 (1967) with corrections noted in J. Fluid Mech. **36**, 193 (1969).

[16]S. K. Bahl, "Stability of viscous flow between two concentric rotating porous cylinders," Def. Sci. J. **20**, 89 (1970).

[17]P. G. Reddy and Y. B. Reddy, "Stability of a non-Newtonian fluid between two concentric rotating cylinders," Def. Sci. J. **26**, 47 (1976).

[18]P. G. Reddy, Y. B. Reddy, and A. G. S. Reddy, "The stability of non-Newtonian fluid between the two rotating porous cylinders (wide gap case)," Def. Sci. J. **28**, 145 (1978).

[19]Although Ref. 18 alludes to the wide gap case in its title, the case that is considered is that for a ratio of inner cylinder radius to outer cylinder radius of 0.95. Typically, "wide gap" analyses consider much smaller radius ratios.

[20]E. M. Sparrow, W. D. Munro, and V. K. Jonsson, "Instability of the flow between rotating cylinders: The wide gap problem," J. Fluid Mech. **20**, 35 (1964).

[21]R. J. Donnelly, K. W. Schwarz, and P. H. Roberts, "Experiments on the stability of viscous flow between rotating cylinders: VI. Finite-amplitude experiments," Proc. R. Soc. London Ser. A **283**, 531 (1965).

[22]M. A. Hasoon and B. W. Martin, "The stability of viscous axial flow in an annulus with a rotating inner cylinder," Proc. R. Soc. London Ser. A **352**, 351 (1977).

[23]N. Gravas and B. W. Martin, "Instability of viscous axial flow in annuli having a rotating inner cylinder," J. Fluid Mech. **86**, 385 (1978).